Amino Acids (2012) 43:1119–1129
DOI 10.1007/s00726-012-1296-9

INVITED REVIEW

Analysis of the *Plasmodium falciparum* proteasome using Blue Native PAGE and label-free quantitative mass spectrometry

Nicole Sessler · Karsten Krug · Alfred Nordheim · Benjamin Mordmüller · Boris Macek

Received: 25 July 2011 / Accepted: 4 April 2012 / Published online: 22 July 2012

Abstract Detailed knowledge of the composition of protein complexes is crucial for the understanding of their structure and function; however, appropriate techniques for compositional analyses of complexes largely rely on elaborate tagging, immunoprecipitation, cross-linking and purification strategies. The proteasome is a prototypical protein complex and therefore an excellent model to assess new methods for protein complex characterisation. Here we evaluated the applicability of Blue Native (BN) PAGE in combination with label-free protein quantification and protein correlation profiling (PCP) for the investigation of proteasome complexes directly from biological samples. Using the purified human 20S proteasome we showed that the approach can accurately detect members of a complex by clustering their gel migration profiles. We applied the approach to address proteasome composition in the schizont stage of the malaria parasite *Plasmodium falciparum*. The analysis, performed in the background of the whole protein extract, revealed that all subunits comigrated and formed a tight cluster with a single maximum, demonstrating presence of a single form of the 20S proteasome. This study shows that BN PAGE in combination with label-free quantification and PCP is applicable to the analysis of multiprotein complexes directly from complex protein mixtures.

Keywords BN PAGE · PCP · Protein complex · LTQ Orbitrap XL · Proteasome · *Plasmodium falciparum*

Abbreviations

BN PAGE	Blue native polyacrylamide gel electrophoresis
MS	Mass spectrometry
PCP	Protein correlation profiling
PAI	Protein abundance index
AUC	Area under the curve
iBAQ	Intensity-based absolute quantification

Introduction

Multiprotein complexes are vital supramolecular assemblies involved in almost every process in the cell. They regulate diverse cell mechanisms, such as protein degradation (proteasome) or protein translation (ribosome). Information on their composition is crucial for understanding of their structure and molecular mechanisms they mediate. Despite of the growing number of studies addressing protein–protein interaction networks (interactomes), determining the exact composition of single complexes is still a challenging task.

The compositional analysis of protein complexes is usually performed by tagging one of the members of the

Electronic supplementary material The online version of this article (doi:10.1007/s00726-012-1296-9) contains supplementary material, which is available to authorized users.

N. Sessler · K. Krug · B. Macek (✉)
Proteome Center Tübingen, Interfaculty Institute for Cell Biology, University of Tübingen, Auf der Morgenstelle 15, 72076 Tübingen, Germany
e-mail: boris.macek@uni-tuebingen.de

N. Sessler · B. Mordmüller
Institute of Tropical Medicine, Universität Tübingen, Wilhelmstr. 27, 72074 Tübingen, Germany

A. Nordheim
Department of Molecular Biology, Interfaculty Institute of Cell Biology, Universität Tübingen, Auf der Morgenstelle 15, 72076 Tübingen, Germany

protein complex, e.g. by His_6-tag (Hochuli et al. 1988), FLAG-tag (Ho et al. 2002) or TAP-tag (Gavin et al. 2002) and performing immunoprecipitation against the tag(s). All proteins that co-precipitate with the targeted protein are assumed to be interactors and therefore potential members of the complex. However, the binding properties of the individual subunits can be influenced by tagging, by overexpression of one member of the complex, by presence or absence of co-factors (e.g. ATP, protease and kinase modulators) or by employed buffer conditions. Since nonspecific interactors may also be present in the precipitate, alternative strategies have to be employed to validate the results.

Alternative method to analyse protein–protein interactions is chemical cross-linking, where functional groups on proteins present in close proximity are linked by cross-linking reagents. Interacting proteins are identified after isolation of the cross-linked complexes by, e.g. mass spectrometry (Maiolica et al. 2007; Gingras et al. 2007). Different strategies can be performed employing different reactive groups, cleavable cross-linkers or cross-linkers with affinity groups (Petrotchenko and Borchers 2010; Leitner et al. 2010); however, the main limitation is the difficulty to control specificity of cross-linking, especially in the background of other cellular proteins.

Protein complexes can also be analysed in their native form. The blue native polyacrylamide gel electrophoresis (BN PAGE) was developed as a method to analyse membrane proteins and protein complexes under native conditions. In BN PAGE, the sample buffer and the cathode buffer are supplemented with Coomassie G-250 to provide a negative charge to proteins and to enable electrophoretic mobility in the gel. Since no SDS is required for migration, the electrophoresis is performed under native conditions. To analyse composition of protein complexes in more detail, SDS PAGE can be performed in a second dimension to separate the members of the complex and to identify the protein spots by western blotting or mass spectrometry (Schägger and von Jagow 1991; Wittig et al. 2006).

The applicability of BN PAGE to the analysis of membrane proteins and protein complexes has been shown in several studies (Eubel et al. 2003; Fandino et al. 2005; Sanders et al. 2007; Wittig and Schägger 2008). Most of the studies employed a fractionation step before analysis (e.g. organelle fractionation), but some demonstrated the applicability of the BN PAGE to whole cell lysates (Camacho-Carvajal et al. 2004).

The protein correlation profiling (PCP) is a computational method first introduced to assign proteins to different organelles in the cell (Andersen et al. 2003; Foster et al. 2006). These studies employed a subcellular fractionation by centrifugation in a sucrose gradient before analysis of the resulting fractions by MS. Protein intensities from adjacent fractions were combined into intensity profiles and correlated with the intensity profiles of marker proteins known to be present in specific organelles. Thus, the PCP requires a prefractionation step before the MS analysis to obtain the intensity profiles. In most studies so far ultracentrifugation was used as fractionation method, but it was shown that BN PAGE can also be applied (Wessels et al. 2009). Assuming that protein complexes stay intact during BN PAGE, PCP may be used to assign identified proteins to multiprotein complexes in protein mixtures by assessing their comigration in the gel.

The 26S proteasome is an essential multiprotein complex in eukaryotes, mainly responsible for the degradation of proteins (Hershko and Ciechanover 1992; Bochtler et al. 1999; Glickman and Ciechanover 2002). It consists of one 20S core complex and two 19S regulatory particles. The 20S proteasome consists of 14 subunits, α_1–α_7 and β_1–β_7; the α- and the β-subunits form a heptameric ring structure, the α_{1-7}-ring and the β_{1-7}-ring. The complete 20S proteasome is formed by the interaction of two α_{1-7}-rings and two β_{1-7}-rings in the order $\alpha_{1-7}\beta_{1-7}\beta_{1-7}\alpha_{1-7}$. This results in a barrel-like structure with a molecular weight of about 700 kDa (Groll et al. 1997).

Malaria, caused by *Plasmodium falciparum,* is worldwide the most important parasitic disease in terms of morbidity and mortality. The high rate of resistance development entails the continuous search for new drugs (Mordmüller and Kremsner 2006) and proteasome inhibitors are one potential novel class of broad-spectrum antimalarials (Kreidenweiss et al. 2008; Tschan et al. 2011). Consequently, detailed information about the target complexes (the proteasome and PfHslV) is important. The genome of *P. falciparum* (strain 3D7) was sequenced in 2002 (Gardner et al. 2002) and showed that the subunits of the 20S proteasome are conserved, with high sequence similarity compared with *Saccharomyces cerevisiae* (Mordmüller et al. 2006) and other eukaryotic organisms (Gille et al. 2003). The structure and composition of the 20S proteasome in the parasite was not studied yet, but due to sequence conservation it is proposed that the structure is similar to the proteasome in human and yeast except for interspersed low complexity regions in subunits β_1, β_3, and β_7 (Mordmüller et al. 2006).

In this study we applied the combination of BN PAGE with label-free protein quantification and PCP to study the proteasome of *P. falciparum* in the schizont stage of the parasite's life cycle. We first used purified human 20S proteasome to validate the applicability of the approach to compositional analysis of the proteasome and, to a lesser extent, to estimation of stoichiometry of complex subunits. By applying the approach to the analysis of the 20S proteasome of *P. falciparum* in the background of complete protein extract, we showed that all 20S subunits comigrate on the BN gel in a tight cluster, pointing to the presence of

only one form of the proteasome in the schizont stage of the life cycle.

Materials and methods

Cultivation of *Plasmodium falciparum*

The *P. falciparum* strain 3D7 was obtained from the Malaria Research and Reference Reagent Resource Center (MR4, Manassas, USA). The parasites were cultured in erythrocytes (blood type 0, Rh.+) and RPMI-1640 medium (PAA, Pasching, Austria) with a hematocrit of 5 %. The parasite cultures were incubated in a humidified atmosphere at 37 °C and in a gaseous environment of 5 % CO_2, 5 % O_2 and 90 % N_2 (Binh et al. 1997). Synchronisation with 5% sorbitol was performed once a week to keep the parasites in a defined stage (Mordmüller et al. 2006).

To prepare a parasite-enriched protein lysate, parasite culture with a high parasitemia (>5 %) in the desired stage was pelleted, the erythrocytes were lysed with 0.15 % saponin in PBS (w/v) and washed until the supernatant was free of haemoglobin (Fry and Beesley 1991). The parasites were lysed using a high salt buffer (20 mM HEPES, 350 mM NaCl, 1 mM $MgCl_2$, 0.5 mM EDTA, 0.1 mM EGTA, 20 % glycerol, 1 % NP-40, pH 7.9) and complete protease inhibitor cocktail (Roche Diagnostics GmbH, Mannheim, Germany). The parasite debris was pelleted and the supernatant containing the cytosolic proteins was collected.

Blue native polyacrylamide gel electrophoresis and western blot

The lysis buffer of the *P. falciparum* lysate was exchanged against BN sample buffer (500 mM Aminocaproic acid, 20 mM Bis–Tris, 2 mM EDTA, 12 mM NaCl, 10 % glycerol, pH 7.0, 4 °C) (Camacho-Carvajal et al. 2004) and complete protease inhibitor cocktail (Roche Diagnostics GmbH, Mannheim, Germany) using 30 kDa Nanoseps (Pall, Dreieich, Germany). Ten micrograms of purified human 20S proteasome (BostonBiochem, Cambridge, USA), optionally supplemented with five proteins, fetuin, α-casein, β-casein, bovine serum albumin and carbonic anhydrase (each 7.5 fmol), was mixed with 0.5 % Coomassie G-250 and applied to a self-casted 6.5 % BN gel. In the second experiment, the same procedure was repeated with 75 µg of the *P. falciparum* lysate. The electrophoresis run was carried out with an cathode buffer (250 mM Tricine, 75 mM Bis–Tris, pH 7.0, 4 °C) supplemented with 0.1 % Coomassie G-250 and an anode buffer (300 mM Bis–Tris, pH 7.0, 4 °C). After one-third of the run the blue cathode buffer was exchanged against cathode buffer without Coomassie and the run was finished (Schägger and von Jagow 1991; Wittig et al. 2006). NativeMark™ (Invitrogen GmbH, Darmstadt, Germany) was used to estimate the size of the complexes.

For the western blot the protein complexes in the BN gel were denatured with 1 % SDS, 1 % β-mercaptoethanol in water (v/v) before transferring onto a nitrocellulose membrane. The plasmodial and the human proteasome were detected with a 20S proteasome antibody (α1,2,3,5,6&7-subunit, clone MCP231, Calbiochem, Darmstadt, Germany) and an anti-mouse IgG HRP-linked secondary antibody (Cell Signaling Technology Inc., Danvers, USA).

Mass spectrometry

The area in the gel containing the 20S proteasome detected by western blot was cut into eight (human proteasome) and twelve slices (plasmodia proteasome), respectively. The gel pieces were destained by washing three times with 10 mM ammonium bicarbonate (ABC)/acetonitrile (ACN) (1:1, v/v). The proteins were reduced with 10 mM DTT in 20 mM ABC (45 min, 56 °C) and alkylated in the dark with 55 mM iodoacetamide in 20 mM ABC (30 min, RT). After washing and dehydration the proteins were digested with 12.5 ng/µl trypsin (sequence grade, Promega GmbH, Mannheim, Germany) in 20 mM ABC (overnight, 37 °C). The resulting peptides were extracted in three subsequent incubation steps with 30 % ACN/3 % TFA, with 80 % ACN/0.5 % acetic acid, and with 100% ACN. The supernatants were combined, ACN was evaporated in a vacuum centrifuge and peptides were desalted using C18 StageTips (Rappsilber et al. 2007; Borchert et al. 2010).

The digested peptide mixtures were separated on an Easy-nanoLC HPLC (Proxeon Biosystems, Odense, Denmark) coupled to a LTQ Orbitrap XL mass spectrometer (Thermo Fisher Scientific, Dreieich, Germany) through a nano-LC–MS interface (Proxeon Biosystems, Odense, Denmark). The separation was performed on a 15-cm fused silica emitter HPLC column, inner diameter of 75 µm (New Objective, Inc., Woburn, USA), which was packed in-house with reversed-phase ReproSil-Pur C18-AQ 3 µm resin (Dr. Maisch GmbH, Ammerbuch, Germany). The samples were injected onto the column in HPLC solvent A (0.5 % acetic acid) at a flow rate of 500 nl/min and subsequently eluted with a 107-min segmented gradient of 2–80 % HPLC solvent B (80 % ACN in 0.5 % acetic acid) at a flow rate of 200 nl/min. The mass spectrometer was operated in a data-dependent mode to switch between MS and MS/MS acquisition. A full scan was acquired in the Orbitrap mass analyser in the mass range of m/z 300–2,000 and a resolution of 60,000. Selected ion monitoring (SIM) scan in the mass range of m/z 350–950 (for human proteasome) and m/z 400–1,000 (for *P. falciparum*

proteasome) was acquired as a survey scan in the Orbitrap mass analyser at a resolution of 60,000 and an accumulation target value of 10^6 charges within a maximal filling time of 1,000 ms (for the human 20S proteasome) and 5×10^5 charges within 1,000 ms (for the plasmodial samples). To improve the mass accuracy the lock mass option of the FT analyzer was enabled (Olsen et al. 2005). The five most intense ions were sequentially isolated and fragmented in the ion trap using collision-induced dissociation (CID) at the CID default settings and at the ion accumulation target value of 5,000. The ions already selected for fragmentation were dynamically excluded from the analysis for 90 s. For quantification of the proteins a label-free quantification approach was performed (see below) and the samples were analysed in technical triplicates. The complete workflow is shown in Fig. 1.

Data analysis and protein correlation profiling

The raw files were processed using the MaxQuant software suite (version 1.0.14.3) (Cox and Mann 2008; Cox et al. 2009). The peak lists of the raw MS spectra were generated with the "Quant" module of the software suite. The second processing step was the database search using the search engine Mascot (version 2.2.0, Matrix Science, Boston, USA) (Perkins et al. 1999) against an in-house assembled target-decoy database (Elias and Gygi 2007). The human database consisted of the IPI human database (version 3.64, 84032 protein entries, EMBL, Hinxton, UK) and 262 commonly observed contaminants; the used plasmodial database consisted of the protein database from PlasmoDB (versions 5.5, 5460 protein entries, or version 6.6, 5446 protein entries, http://plasmodb.org/plasmo/; Aurrecoechea et al. 2009) and 262 commonly observed contaminants. The database search was performed with carbamidomethylation (Cys) as fixed modification, oxidation (Met) and acetylation (protein N termini) as variable modifications. The mass tolerances for the precursor and fragment ions were set to 7 ppm and 0.5 Da, respectively. In the third step the "Identify" module was used to parse the Mascot results. Posterior error probabilities (PEP) for each identified MS/MS spectra were calculated by the software and used to control the false discovery rates (FDR) according to the target-decoy approach. FDRs were set to 1 % on both protein groups and peptide level. Furthermore, the "Identify" module performed the label-free quantification by adjusting the corresponding protein intensities across the gel slices measured in triplicates (Luber et al. 2010). The adjusted intensities were used for PCP. For the reprocessing of the plasmodial dataset, the database search was performed using the combined *P. falciparum* (version 8.0, 5491 protein entries, http://plasmodb.org/plasmo/) and human (version 3.84, 90166 protein entries, EMBL, Hinxton, UK) protein databases including the 262 commonly observed contaminants. All other parameters for the search using the MaxQuant software (version 1.0.14.3) were used as described above.

The PCP was performed by plotting the $\log_{10}$-transformed intensities of the proteasomal subunits (the summed intensity of all identified peptides) across the slices of the BN gel (Andersen et al. 2003; Foster et al. 2006). For the purified human 20S proteasome the raw (non-adjusted) intensities were used for the PCP, because the dataset was too small for label-free quantification. The PCP of the plasmodial proteasome was performed using the adjusted intensities. The resulting intensity profiles were compared with each other to detect any correlation between the proteins.

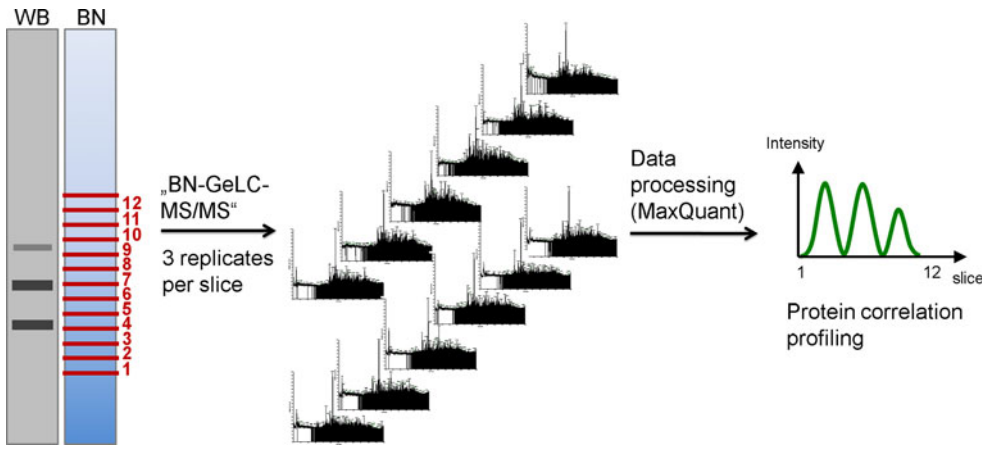

Fig. 1 Schematic workflow of BN PAGE in combination with label-free quantitative MS. The protein mixture of interest is separated in two lanes on a BN PAGE. One lane is subjected to western blotting, whereas the other is cut into slices; proteins are in-gel digested and the resulting peptides are measured on a mass spectrometer. The protein intensity profiles are derived from intensities in individual (adjacent) slices. The intensity profiles are subjected to protein correlation profiling to detect comigrating proteins, which are likely members of a complex

Unsupervised cluster analysis of protein intensity profiles across the BN gel slices was done in R (R Development Core Team 2011). All protein groups with at least one adjusted intensity value across the twelve slices were included into the clustering. Intensity profiles of protein groups were transformed to standard scores (z-scores) and clustered using the *k*-means algorithm in conjunction with the consensus clustering method (Monti et al. 2003) implemented in the R-package "ConsensusClustPlus". Cluster numbers between two and twelve were used to perform clustering on the protein intensity profiles. To assess the robustness of resulting clusters, 1,000 iterations of the *k*-means algorithm were performed on sub-samplings containing 80 % of the original data. From the iterations the algorithm has calculated an item score for each cluster member (the relative frequency of each cluster member belonging to the same cluster). To quantify the overall robustness of a cluster the average item consensus was calculated as the cluster consensus. The optimal cluster number was determined visually as described in Monti et al. (2003).

Determination of stoichiometry

The stoichiometry of the proteasome subunits was determined as ratio of their normalised abundances. Three different approaches were used for abundance determination: the protein abundance index (PAI) (Rappsilber et al. 2002), an adaptation of the intensity-based absolute quantification (iBAQ) (Schwanhäusser et al. 2011) and quantification based on the calculation of the area under the curve (AUC). The theoretically observable number of peptides per protein was used for normalisation in all three approaches. To that end, the sequences of the 14 subunits were digested in silico using the program GPMAW (version 8.1, Lighthouse data, Odense, Denmark). For in silico digestion trypsin was defined as enzyme and one missed cleavages was allowed. The *m*/*z* values of doubly and triply charged ions in the mass range of *m*/*z* 350–950 for the human proteasome subunits and *m*/*z* 400-1,000 for the *P. falciparum* proteasome subunits were used for the calculation of the theoretical number of peptides per protein.

For calculation of PAI, the number of observed peptides for every subunit was determined using the evidence table of the MaxQuant output. The PAI value for every subunit was calculated as number of observed peptides divided by number of theoretical (observable) peptides.

For quantification using the iBAQ approach, two different intensity values were used: the total protein intensity and the sum of the intensities of the three most intensive peptides (TOP3). The intensity values of the subunits were divided by the theoretical number of peptides to result in the iBAQ values.

The AUC of the normalised intensity profile of every subunit was calculated using the software Origin (OriginLab Corporation, Northampton, USA). For every subunit the AUC value was normalised by dividing by the corresponding theoretical number of peptides.

The standard deviation for each method was estimated based on a sample using the following formula (with $n = 14$ for the 14 proteasomal subunits):

$$\mathrm{StDev} = \sqrt{\frac{\sum (x - \bar{x})^2}{(n-1)}}.$$

Results

The human 20S proteasome

In this study we applied the BN PAGE in combination with label-free quantification and PCP to study composition of the *P. falciparum* proteasome directly from the whole protein extract.

We first tested the applicability of the approach by performing compositional analysis of the human 20S proteasome. Commercially obtained purified human 20S proteasome was separated in two BN PAGE lanes; one lane was blotted and probed with an antibody against the α-subunits of the 20S proteasome, whereas the other lane was cut into eight equal slices in the area of the detected proteasome. Only one band could be detected on the Coomassie stained BN gel of the human proteasome (Fig. 2a). The western blot analysis showed one strong signal on the position of the 720-kDa marker (Fig. 2b), which corresponds to the molecular weight of the intact 20S proteasome. After protein digestion in the eight excised gel slices, the extracted peptide mixtures were analysed in triplicates with LC–MS/MS on an LTQ Orbitrap XL. The spectra were acquired using broad-range selected ion monitoring (SIM) as the survey scan in the *m*/*z* range of 350–950 Th. In a SIM scan, the required number of ions is accumulated only in the selected mass range which enhances the sensitivity and the dynamic range. In the *m*/*z* range of 350–950 peptides from all of the 20S proteasome subunits were expected to be detected. The MS data were processed using the MaxQuant software and quantified using the integrated label-free algorithm. In total, 52 human protein groups were identified, including all 14 subunits of the 20S proteasome, as well as isoforms of the subunits α_7 and β_5 and four subunits of the immuno-proteasome, β_{1i}, β_{2i}, β_{5i} and β_{5t}.

The intensity profiles of the 14 proteasomal subunits were constructed from protein intensities in adjacent gel slices (Fig. 2c and Online Resource 1a and 1b). The alignment of the western blot (signal in slice 3 to slice 5)

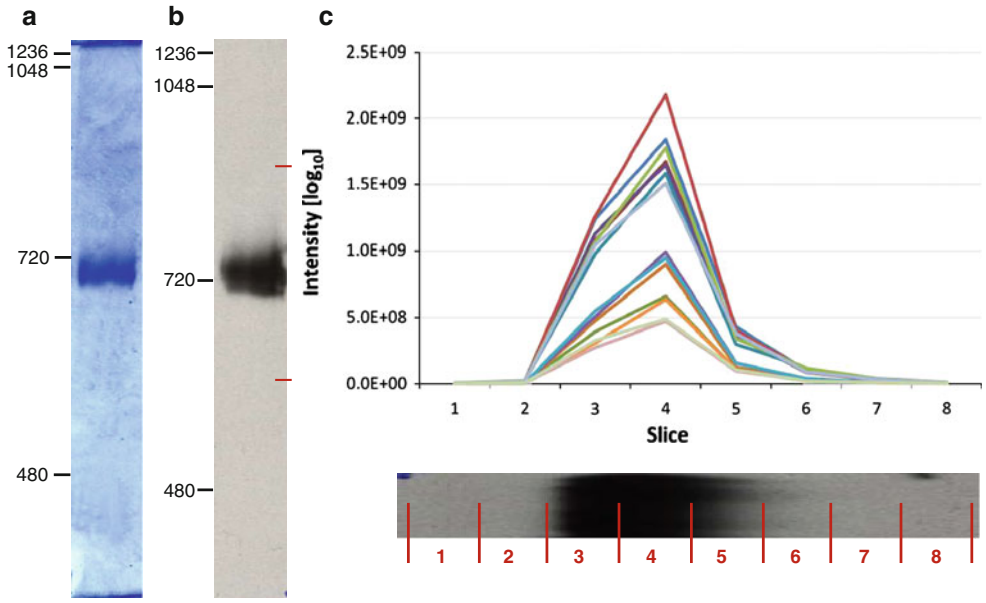

Fig. 2 Analysis of the purified human 20S proteasome. **a** Coomassie stained BN gel of the human proteasome. **b** Western blot of the proteasome separated on a BN gel using an antibody against the proteasomal α-subunits. The *marks* indicate the excised area of the gel lane for the MS analysis. **c** Intensity profiles of all 14 subunits of the human 20S proteasome plotted across analysed BN gel slices. The aligned western blot of the BN gel shows the correlation between the maximum of the intensity profiles and antibody signal of the proteasomal subunits

with the intensity profiles revealed a strong correlation between the antibody staining and the intensity profiles obtained without application of the label-free algorithm. All 14 intensity profiles showed a maximum in slice 4 demonstrating that the subunits comigrated in the BN gel and were therefore members of the same complex (Fig. 2c). Interestingly, despite of equimolar amounts of the 20S subunits, their intensities differed by up to one order of magnitude. As expected, the intensity profiles obtained after application of the label-free algorithm did not show any correlation, demonstrating that the label-free quantification requires more data points (more complex mixture) for reliable signal intensity adjustment (Online Resource 1b).

We therefore performed another experiment where the purified human 20S proteasome was supplemented with five proteins to increase the complexity of the sample (fetuin, α-casein, β-casein, bovine serum albumin and carbonic anhydrase) and analysed as described above. In this sample 82 protein groups were identified, including the five added proteins, 14 subunits of the human 20S proteasome, isoforms of the subunits α_7 and β_5 and four subunits of the immuno-proteasome, β_{1i}, β_{2i}, β_{5i} and β_{5t}. A summary of the number of identified proteins in the two experiments is shown in Table 1. The adjusted intensity profiles after application of the MaxQuant label-free algorithm improved significantly in the more complex mixture, showing one maximum and good correlation with the BN gel image (Online Resource 1c and 1d).

Table 1 Overview of the experiments performed on the purified human 20S proteasome

Exp.	Scan type	Detected human protein groups	Detected 20S subunits
20S	SIM scan	52	14 + 6
20S + five proteins	SIM scan	82	14 + 6

All 14 subunits of the 20S proteasome as well as isoforms α7 and β5 and four subunits of the immuno-proteasome, β1i, β2i, β5i, and β5t were detected

The human 20S proteasome is a good model to test the accuracy of subunit stoichiometry determination since its every subunit is present in equimolar amount. As the subunits differ in length and number of peptides, additional quantification method needs to be applied for direct comparison of their abundances. The measured intensities of the detected 20S proteasome subunits differed to up to one order of magnitude; therefore, we applied three different label-free quantification methods to determine relative abundance of the detected subunits: PAI, AUC and a modified version of iBAQ.

Determination of abundances with PAI resulted in relative abundance values in the range from 0.1216 (β_5) to 1 (β_3), with the standard deviation of 0.2556 (Fig. 3a). The relative AUC values for the proteasomal subunits ranged from 0.3641 (β_7) to 1 (α_7) and resulted in the standard deviation of 0.2304 (Fig. 3b). Application of iBAQ (all

peptides) resulted in relative values from 0.3647 (β_7) to 1 (β_5) with a standard deviation of 0.2306 (Fig. 3c). The relative abundance values obtained using iBAQ TOP3 showed the minimal variation and ranged from 0.5464 (β_7) to 1 (β_5) with the standard deviation of 0.1324 (Fig. 3d). These data demonstrate that the employed label-free quantification methods managed to decrease the measured subunit intensity variation from tenfold to twofold, indicating that this approach can be potentially used to assess the subunit stoichiometry. However, further analyses on complexes with unequimolar stoichiometries and subunits of markedly different sizes will be needed to resolve the usefulness of the approach for subunit stoichiometry determination. The calculation of the abundance values using AUC and iBAQ of all proteins resulted in a strong correlation, most likely due to the fact that quantification in both methods was based on the total protein intensities.

20S proteasome of *Plasmodium falciparum*

After establishing that the BN PAGE in combination with PCP and label-free quantification can reliably identify subunits of the purified human proteasome, we applied the approach to study the composition of the proteasome of *P. falciparum* in the schizont stage of the parasite's life cycle. To that end, parasites in schizont stage were harvested, lysed and the lysate was loaded in three lanes of a BN gel. A parasite lysate separated on a BN gel and stained with Coomassie indicated a more complex sample as the purified human 20S proteasome, but no clear bands were visible (Fig. 4a). For detection of the proteasome by western blot, two lanes of the BN gel were transferred onto a nitrocellulose membrane and incubated with the antibody against the α-subunits of the human 20S proteasome, which can also detect the plasmodial 20S proteasome (Mordmüller et al. 2006). Based on the known sequences and with the assumption that the complex consists of two α-rings and two β-rings, the calculated size of the plasmodial 20S proteasome is 764 kDa. However, the western blot analysis resulted in detection of three distinct signals at different molecular weights (from about 550 kDa to about 750 kDa) and with different intensities, indicating the presence of three forms of the proteasome (Fig. 4b). In the remaining lane of the BN gel, the area containing the proteasome was cut into twelve equal slices, the proteins in the slices were digested and the resulting peptide mixtures were analysed by MS. The sample analysis was done in biological triplicates; two experiments were performed using normal survey scans (mass range *m/z* 300–2,000) before MS/MS fragmentation of the ions. The third experiment was carried out using a SIM scan as a survey scan in the range of *m/z* 400–1,000. A summary of the applied MS acquisition methods and the numbers of identified proteins in the three experiments is shown in Table 2. In every experiment all 14 subunits of the 20S proteasome were detected and in the second experiment additional twelve subunits of the proteasome regulatory particle were

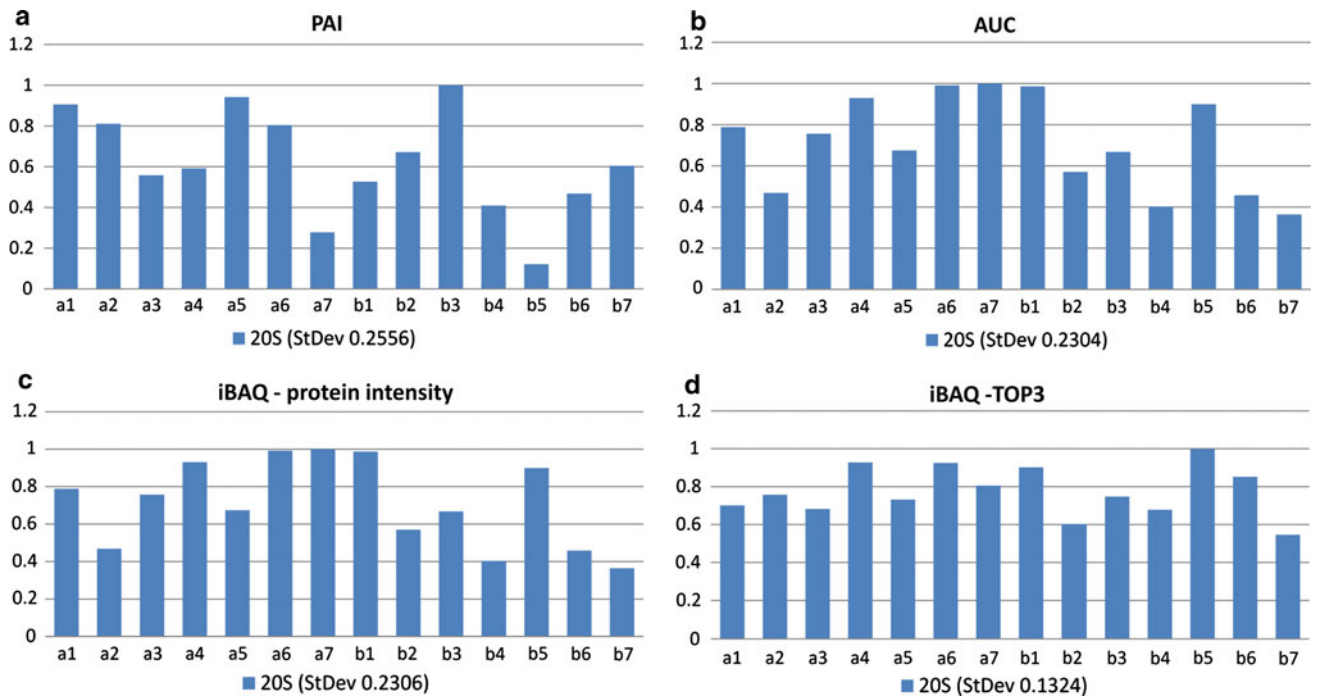

Fig. 3 Determination of stoichiometry of the purified human 20S proteasome. Three different label-free quantification methods (PAI, AUC and two versions of iBAQ) were used. The standard deviation is given in the legend

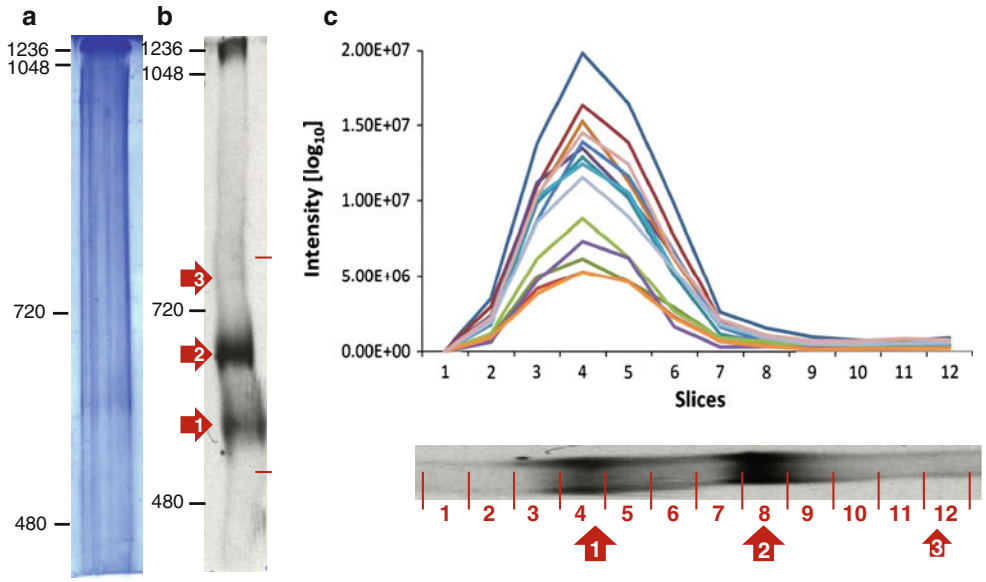

Fig. 4 Analysis of the *P. falciparum* 20S proteasome. **a** The plasmodial lysate was separated on a BN gel and stained with Coomassie. **b** For western blot analysis the parasite lysate was separated on a BN PAGE and the detection using an antibody against the human proteasomal α-subunits revealed three distinct bands, which are marked. The additional *marks* indicate the excised area of the gel for the MS analysis. **c** The overlay of the intensity profiles of 14 subunits of the *P. falciparum* 20S proteasome and the western blot reveals the correlation between the maximum of the profiles and the signal in slice 4. This points to the fact that signal 1 corresponds to the 20S proteasome, but signal 2 and signal 3 do not

Table 2 Overview of the three experiments performed on the whole cell lysates of *P. falciparum*

Exp.	Scan type	Detected plasmodial protein groups	Detected 20S subunits	Detected subunits of regulatory particle
1	Full scan	286	14	–
2	Full scan	380	14	12
3	SIM scan	246	14	–

identified. The identified protein groups of all five experiments (human and plasmodial 20S proteasome) are summarised in Online resource 2.

The intensity profiles of the 20S proteasomal subunits were derived from adjusted protein intensities of adjacent slices in the BN gel. The resulting intensity profiles of the 14 subunits showed the same trend with one maximum. An overlay of the intensity profiles and the western blot showed a correlation between the intensity maximum and the first signal in western blot (Fig. 4c). Notably, the western blot signal 2 and signal 3 had no corresponding maxima in the intensity profiles of the 20S subunits. These data demonstrate that all subunits of the 20S proteasome comigrate in the BN gel and are therefore present in a single complex. The two additional signals in the western blot were likely due to cross-reactivity of the antibody with the subunits of the regulatory particle of the proteasome (see below). The summary of the number of identified peptides of the proteins and their corresponding intensities in the analysed slices of the BN gel is given in Online Resource 3. We note that the apparent position of the detected *P. falciparum* 20S proteasome was at approximately 550 kDa. To avoid any potential confusion due to a possible contamination with the host (human) proteasome, we re-analysed the MS data by searching against the combined *P. falciparum* and human protein databases. The result indicated that the human proteasome was indeed present, but at approximately 100-fold lower intensities. Importantly, the human proteasome subunits showed the same co-migration profiles as *P. falciparum* subunits, with maxima at 550 kDa (Online Resource 4). Since the position of the purified human 20S proteasome was at ca. 700 kDa (Fig. 2b), we conclude that the migration during analysis of the *P. falciparum* lysate must have been altered by the complexity of the sample.

We validated these results by performing unsupervised clustering of the intensity profiles of 20S proteasome subunits using consensus clustering (Monti et al. 2003). The 314 quantified proteins detected in experiment 2 clustered into six clusters (Online Resource 5 and 6). Only

one cluster showed a very good correlation between the intensity profiles (cluster 5), resulting in a consensus value of 0.914. This cluster contained 21 proteins, among them all 14 subunits of the 20S proteasome and seven additional proteins (Fig. 5). Although this was the only strong cluster containing a single complex (the 20S proteasome), other known complexes were detected in the analysed gel region. For example, the low molecular weight rhoptry (RAP) complex was identified in Cluster 2, the high molecular weight rhoptry (RhopH) complex and the mitochondrial signal peptide processing complex were detected in Cluster 1. Importantly, the profiles of the members of these complexes showed a good correlation indicating a co-migration (Online Resource 7). The proteasome was singled out in one cluster mostly due to the fact that it consists of many (14) co-migrating subunits.

The intensity profiles of the ten subunits of the proteasome regulatory particle quantified in experiment 2 showed high variability, most likely due to their low signal intensity. Their maxima were distributed over all slices and some of the profiles showed more than one maximum (Online Resource 8). No correlation between the profiles of the regulatory and 20S proteasome subunits could be observed. Some of the subunits have shown three maxima in their intensity profiles, so it is likely that the antibody used in western blot cross-reacted with these subunits.

As in the case of the human proteasome, three different label-free quantification methods were used to determine the subunit stoichiometry: PAI, AUC and iBAQ (total protein intensity and iBAQ TOP3). The number of theoretical peptides was in this case calculated with one missed cleavage, because only about 10 % miss-cleaved peptides were detected in each dataset. As demonstrated on human proteasome, the values derived by iBAQ TOP3 method were the best, showing a twofold difference in the relative abundance of equimolar subunits; all other methods resulted in a higher change (Online Resource 9).

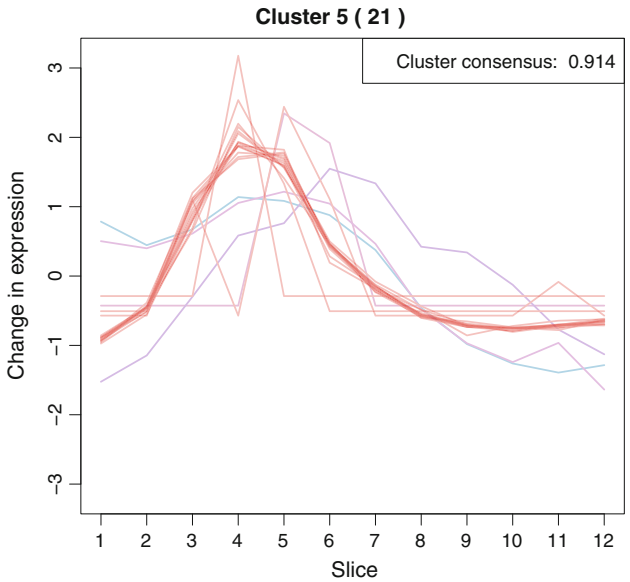

Fig. 5 Unsupervised consensus *k*-means clustering. Cluster 5 contained 21 proteins, all 14 proteasomal subunits and seven additional proteins. The cluster consensus value for this cluster 0.914 indicates a high stability. The seven additional profiles, which were slightly different from others, could be assigned to additional proteins

Discussion

In this study we combined BN PAGE with label-free quantitative mass spectrometry and protein correlation profiling to analyze the *P. falciparum* proteasome from the schizont stage of the parasite's life cycle. The advantage of the applied approach is the possibility to analyse protein complexes in the background of very complex protein mixtures, such as whole protein extracts, without the need for purification of the complex. The only prerequisite for PCP is a protein fractionation step before MS analysis, which in our study was the BN PAGE. Since BN PAGE preserves strong protein complexes during separation (i.e. they migrate in tight clusters), the members of the complex must have identical migration profiles on the gel. Therefore, PCP applied to MS intensity profiles of proteins detected in a specific gel region can identify the members of the complex. A similar method was described recently by Wessels and co-workers (Wessels et al. 2009) for analysis of the oxidative phosphorylation complexes I–V in isolated human mitochondria. However, in the case of the plasmodial 20S proteasome the protein complex is not confined to an organelle, making its purification or enrichment difficult. In addition, the amount of proteins that can be obtained from a plasmodial culture is limited and contamination by host proteins cannot be excluded—even if purification of the protein complex of interest is feasible, it is likely that the amount of the purified protein complex would be too low for the analysis. The method described here is therefore also applicable to organisms/cell cultures with a low protein yield and high complexity.

We used the human 20S proteasome to validate the approach because its composition and structure are well studied and subunit sequences are conserved between *P. falciparum* and human. The experiments on the human 20S proteasome demonstrated that the approach is able to detect the complex and, as expected, that a mixture of higher complexity is beneficial for label-free quantification. We chose to use the label-free quantification prior to PCP as it was shown that the label-free algorithm effectively adjusts run-to-run differences in measured protein intensities (Luber et al. 2010), which is especially important for analysis of low-abundant proteins.

Interestingly, despite of their similar sizes and equimolar amounts, the measured protein intensities of the 20S proteasome subunits showed a high variability—up to one order of magnitude. We therefore used several approaches to estimate relative abundances of the subunits. The modification of iBAQ method, considering the intensities of three most intense peptides instead all peptides, showed the best performance by decreasing this difference to twofold; however, this is still not sufficiently precise to routinely determine stoichiometries of complex subunits.

We applied BN PAGE with label-free quantitative mass spectrometry to the analysis of the plasmodial lysate from the schizont stage, where our initial western blot analysis using an antibody against the α-subunits of the 20S proteasome showed three distinct signals after separation by BN PAGE. The observed differences on the blot were too low to correspond to the size of the 20S proteasome in complex with one and/or two of the regulatory particles, which indicated a presence of additional forms of the proteasome. This was unusual, since to our knowledge there were no reports of different forms of the 20S proteasome in *P. falciparum*.

As expected, our approach demonstrated that all 20S subunits had only one maximum and the overlay of the western blot and the intensity profiles revealed a clear correlation of only one signal of the western blot and the intensity profiles. We therefore concluded that the signal with the lowest molecular weight in western blot corresponded to the 20S proteasome and that the other two signals were possible due to cross-reactivity of the antibody with some subunits of the regulatory particles.

It has to be noted that the approach presented in this study has obvious limitations: only complexes strong enough to "survive" the BN PAGE treatment can be analysed and the resolution of the PCP may be insufficient in the analysis of complexes with very similar masses. As shown here, the approach also has a very limited applicability to determination of the subunit stoichiometry. However, despite these shortcomings this approach opens up new possibilities in the analysis of protein complexes. One, for example, is the measurement of the on-target effect of compounds designed to interfere with functions of the protein complex. In addition, the approach can be used for systematic identification of protein complexes in organisms such as *P. falciparum*, where low amounts of starting material and contamination by host proteins present a major challenge to the compositional analysis of protein complexes.

Acknowledgments The authors wish to thank Dr. Tobias Lamkemeyer and Dr. Rolf Fendel for helpful discussions in the initial stages of the project. This study was supported by the Landesstiftung BW (Juniorprofessoren-Programm), DFG and PRIME-XS (to Boris Macek).

Conflict of interest The authors declare no conflict of interest.

References

Andersen JS, Wilkinson CJ, Mayor T, Mortensen P, Nigg EA, Mann M (2003) Proteomic characterization of the human centrosome by protein correlation profiling. Nature 426(6966):570–574. doi:10.1038/nature02166

Aurrecoechea C, Brestelli J, Brunk BP, Dommer J, Fischer S, Gajria B, Gao X, Gingle A, Grant G, Harb OS, Heiges M, Innamorato F, Iodice J, Kissinger JC, Kraemer E, Li W, Miller JA, Nayak V, Pennington C, Pinney DF, Roos DS, Ross C, Stoeckert CJ Jr., Treatman C, Wang H (2009) Plasmodb: a functional genomic database for malaria parasites. Nucleic Acids Res 37 (Database issue):D539–543. doi:10.1093/nar/gkn814

Binh VQ, Luty AJ, Kremsner PG (1997) Differential effects of human serum and cells on the growth of *Plasmodium falciparum* adapted to serum-free in vitro culture conditions. Am J Trop Med Hyg 57(5):594–600

Bochtler M, Ditzel L, Groll M, Hartmann C, Huber R (1999) The proteasome. Annu Rev Biophys Biomol Struct 28:295–317. doi:10.1146/annurev.biophys.28.1.295

Borchert N, Dieterich C, Krug K, Schütz W, Jung S, Nordheim A, Sommer RJ, Macek B (2010) Proteogenomics of *Pristionchus pacificus* reveals distinct proteome structure of nematode models. Genome Res 20(6):837–846. doi:10.1101/gr.103119.109

Camacho-Carvajal MM, Wollscheid B, Aebersold R, Steimle V, Schamel WW (2004) Two-dimensional blue native/SDS gel electrophoresis of multi-protein complexes from whole cellular lysates: a proteomics approach. Mol Cell Proteomics 3(2): 176–182. doi:10.1074/mcp.T300010-MCP200

Cox J, Mann M (2008) Maxquant enables high peptide identification rates, individualized p.p.b.-range mass accuracies and proteome-wide protein quantification. Nat Biotechnol 26(12):1367–1372. doi:10.1038/nbt.1511

Cox J, Matic I, Hilger M, Nagaraj N, Selbach M, Olsen JV, Mann M (2009) A practical guide to the maxquant computational platform for SILAC-based quantitative proteomics. Nat Protoc 4(5):698–705. doi:10.1038/nprot.2009.36

Elias JE, Gygi SP (2007) Target-decoy search strategy for increased confidence in large-scale protein identifications by mass spectrometry. Nat Methods 4(3):207–214.doi:10.1038/nmeth1019

Eubel H, Jänsch L, Braun HP (2003) New insights into the respiratory chain of plant mitochondria. Supercomplexes and a unique composition of complex ii. Plant Physiol 133(1):274–286

Fandino AS, Rais I, Vollmer M, Elgass H, Schägger H, Karas M (2005) LC-nanospray-MS/MS analysis of hydrophobic proteins from membrane protein complexes isolated by blue-native electrophoresis. J Mass Spectrom 40(9):1223–1231. doi:10.1002/jms.903

Foster LJ, de Hoog CL, Zhang Y, Xie X, Mootha VK, Mann M (2006) A mammalian organelle map by protein correlation profiling. Cell 125(1):187–199. doi:10.1016/j.cell.2006.03.022

Fry M, Beesley JE (1991) Mitochondria of mammalian *Plasmodium* spp. Parasitology 102(Pt 1):17–26

Gardner MJ, Hall N, Fung E, White O, Berriman M, Hyman RW, Carlton JM, Pain A, Nelson KE, Bowman S, Paulsen IT, James K, Eisen JA, Rutherford K, Salzberg SL, Craig A, Kyes S, Chan MS, Nene V, Shallom SJ, Suh B, Peterson J, Angiuoli S, Pertea M, Allen J, Selengut J, Haft D, Mather MW, Vaidya AB, Martin DM, Fairlamb AH, Fraunholz MJ, Roos DS, Ralph SA, McFadden GI, Cummings LM, Subramanian GM, Mungall C, Venter JC, Carucci DJ, Hoffman SL, Newbold C, Davis RW, Fraser CM, Barrell B (2002) Genome sequence of the human

malaria parasite *Plasmodium falciparum*. Nature 419(6906): 498–511. doi:10.1038/nature01097

Gavin AC, Bosche M, Krause R, Grandi P, Marzioch M, Bauer A, Schultz J, Rick JM, Michon AM, Cruciat CM, Remor M, Hofert C, Schelder M, Brajenovic M, Ruffner H, Merino A, Klein K, Hudak M, Dickson D, Rudi T, Gnau V, Bauch A, Bastuck S, Huhse B, Leutwein C, Heurtier MA, Copley RR, Edelmann A, Querfurth E, Rybin V, Drewes G, Raida M, Bouwmeester T, Bork P, Seraphin B, Kuster B, Neubauer G, Superti-Furga G (2002) Functional organization of the yeast proteome by systematic analysis of protein complexes. Nature 415(6868): 141–147. doi:10.1038/415141a

Gille C, Goede A, Schloetelburg C, Preissner R, Kloetzel PM, Gobel UB, Frommel C (2003) A comprehensive view on proteasomal sequences: Implications for the evolution of the proteasome. J Mol Biol 326 (5):1437–1448. pii:S0022283602014705

Gingras AC, Gstaiger M, Raught B, Aebersold R (2007) Analysis of protein complexes using mass spectrometry. Nat Rev Mol Cell Biol 8(8):645–654. doi:10.1038/nrm2208

Glickman MH, Ciechanover A (2002) The ubiquitin-proteasome proteolytic pathway: destruction for the sake of construction. Physiol Rev 82(2):373–428. doi:10.1152/physrev.00027.2001

Groll M, Ditzel L, Lowe J, Stock D, Bochtler M, Bartunik HD, Huber R (1997) Structure of 20S proteasome from yeast at 2.4 A resolution. Nature 386(6624):463–471. doi:10.1038/386463a0

Hershko A, Ciechanover A (1992) The ubiquitin system for protein degradation. Annu Rev Biochem 61:761–807. doi:10.1146/annurev.bi.61.070192.003553

Ho Y, Gruhler A, Heilbut A, Bader GD, Moore L, Adams SL, Millar A, Taylor P, Bennett K, Boutilier K, Yang L, Wolting C, Donaldson I, Schandorff S, Shewnarane J, Vo M, Taggart J, Goudreault M, Muskat B, Alfarano C, Dewar D, Lin Z, Michalickova K, Willems AR, Sassi H, Nielsen PA, Rasmussen KJ, Andersen JR, Johansen LE, Hansen LH, Jespersen H, Podtelejnikov A, Nielsen E, Crawford J, Poulsen V, Sorensen BD, Matthiesen J, Hendrickson RC, Gleeson F, Pawson T, Moran MF, Durocher D, Mann M, Hogue CW, Figeys D, Tyers M (2002) Systematic identification of protein complexes in *Saccharomyces cerevisiae* by mass spectrometry. Nature 415(6868):180–183. doi:10.1038/415180a

Hochuli E, Bannwarth W, Dobeli H, Gentz R, Stuber D (1988) Genetic approach to facilitate purification of recombinant proteins with a novel metal chelate adsorbent. Nat Biotech 6(11): 1321–1325

Kreidenweiss A, Kremsner PG, Mordmüller B (2008) Comprehensive study of proteasome inhibitors against *Plasmodium falciparum* laboratory strains and field isolates from gabon. Malar J 7:187. doi:10.1186/1475-2875-7-187

Leitner A, Walzthoeni T, Kahraman A, Herzog F, Rinner O, Beck M, Aebersold R (2010) Probing native protein structures by chemical cross-linking, mass spectrometry, and bioinformatics. Mol Cell Proteomics 9(8):1634–1649. doi:10.1074/mcp.R000001-MCP201

Luber CA, Cox J, Lauterbach H, Fancke B, Selbach M, Tschopp J, Akira S, Wiegand M, Hochrein H, O'Keeffe M, Mann M (2010) Quantitative proteomics reveals subset-specific viral recognition in dendritic cells. Immunity 32(2):279–289. doi:10.1016/j.immuni.2010.01.013

Maiolica A, Cittaro D, Borsotti D, Sennels L, Ciferri C, Tarricone C, Musacchio A, Rappsilber J (2007) Structural analysis of multiprotein complexes by cross-linking, mass spectrometry, and database searching. Mol Cell Proteomics 6(12):2200–2211. doi:10.1074/mcp.M700274-MCP200

Monti S, Tamayo P, Mesirov J, Golub T (2003) Consensus clustering: a resampling-based method for class discovery and visualization of gene expression microarray data. Mach Learn 52(1–2):91–118

Mordmüller B, Kremsner PG (2006) Malarial parasites versus antimalarials: never-ending rumble in the jungle. Curr Mol Med 6(2):247–251

Mordmüller B, Fendel R, Kreidenweiss A, Gille C, Hurwitz R, Metzger WG, Kun JF, Lamkemeyer T, Nordheim A, Kremsner PG (2006) Plasmodia express two threonine-peptidase complexes during asexual development. Mol Biochem Parasitol 148(1):79–85. doi:10.1016/j.molbiopara.2006.03.001

Olsen JV, de Godoy LM, Li G, Macek B, Mortensen P, Pesch R, Makarov A, Lange O, Horning S, Mann M (2005) Parts per million mass accuracy on an orbitrap mass spectrometer via lock mass injection into a c-trap. Mol Cell Proteomics 4(12): 2010–2021. doi:10.1074/mcp.T500030-MCP200

Perkins DN, Pappin DJ, Creasy DM, Cottrell JS (1999) Probability-based protein identification by searching sequence databases using mass spectrometry data. Electrophoresis 20(18):3551–3567. doi:10.1002/(SICI)1522-2683(19991201)20:18<3551:AID-ELPS3551>3.0.CO;2-2

Petrotchenko EV, Borchers CH (2010) Crosslinking combined with mass spectrometry for structural proteomics. Mass Spectrom Rev 29(6):862–876. doi:10.1002/mas.20293

R Development Core Team (2011) R: A language and environment for statistical computing. R Foundation for Statistical Computing, Vienna

Rappsilber J, Ryder U, Lamond AI, Mann M (2002) Large-scale proteomic analysis of the human spliceosome. Genome Res 12(8):1231–1245. doi:10.1101/gr.473902

Rappsilber J, Mann M, Ishihama Y (2007) Protocol for micro-purification, enrichment, pre-fractionation and storage of peptides for proteomics using stagetips. Nat Protoc 2(8):1896–1906. doi:10.1038/nprot.2007.261

Sanders PR, Cantin GT, Greenbaum DC, Gilson PR, Nebl T, Moritz RL, Yates JR 3rd, Hodder AN, Crabb BS (2007) Identification of protein complexes in detergent-resistant membranes of *Plasmodium falciparum* Schizonts. Mol Biochem Parasitol 154(2): 148–157. doi:10.1016/j.molbiopara.2007.04.013

Schägger H, von Jagow G (1991) Blue native electrophoresis for isolation of membrane protein complexes in enzymatically active form. Anal Biochem 199(2):223–231

Schwanhäusser B, Busse D, Li N, Dittmar G, Schuchhardt J, Wolf J, Chen W, Selbach M (2011) Global quantification of mammalian gene expression control. Nature 473(7347):337–342. doi:10.1038/nature10098

Tschan S, Mordmüller B, Kun JF (2011) Threonine peptidases as drug targets against malaria. Expert Opin Ther Targets. doi:10.1517/14728222.2011.555399

Wessels HJ, Vogel RO, van den Heuvel L, Smeitink JA, Rodenburg RJ, Nijtmans LG, Farhoud MH (2009) LC-MS/MS as an alternative for SDS-PAGE in blue native analysis of protein complexes. Proteomics 9(17):4221–4228. doi:10.1002/pmic.200900157

Wittig I, Schägger H (2008) Features and applications of blue-native and clear-native electrophoresis. Proteomics 8(19):3974–3990. doi:10.1002/pmic.200800017

Wittig I, Braun HP, Schägger H (2006) Blue native page. Nat Protoc 1(1):418–428. doi:10.1038/nprot.2006.62